RESEARCH ARTICLE

Estimating forest uniformity in *Eucalyptus* spp. and *Pinus taeda* L. stands using field measurements and structure from motion point clouds generated from unmanned aerial vehicle (UAV) data collection

Ângela M. K. Hentz[1], Carlos A. Silva[2], Ana P. Dalla Corte[1], Sylvio P. Netto[1], Michael P. Strager[3], and Carine Klauberg[4]

[1]Federal University of Paraná, Dept. of Forest Science, Av., Prefeito Lothário Meissner, 632, Curitiba, Paraná, 80210-170 Brazil. [2]University of Idaho, Dept. of Natural Resources and Society, College of Natural Resources, 875 Perimeter Drive, Moscow, Idaho, 83843 USA. [3]West Virginia University, Division of Resource Management, Davis College of Agriculture, Natural Resources & Design, 333 Evansdale Drive, Morgantown, West Virginia, 26505 USA. [4]US Forest Service, Rocky Mountain Research Station-RMRS, 1221 South Main Street, Moscow, Idaho, 83843 USA.

Abstract

Aim of study: In this study we applied 3D point clouds generated by images obtained from an Unmanned Aerial Vehicle (UAV) to evaluate the uniformity of young forest stands.

Area of study: Two commercial forest stands were selected, with two plots each. The forest species studied were *Eucalyptus* spp. and *Pinus taeda* L. and the trees had an age of 1.5 years.

Material and methods: The individual trees were detected based on watershed segmentation and local maxima, using the spectral values stored in the point cloud. After the tree detection, the heights were calculated using two approaches, in the first one using the Digital Surface Model (DSM) and a Digital Terrain Model, and in the second using only the DSM. We used the UAV-derived heights to estimate an uniformity index.

Main results: The trees were detected with a maximum 6% of error. However, the height was underestimated in all cases, in an average of 1 and 0.7 m for *Pinus* and *Eucalyptus* stands. We proposed to use the models built herein to estimate tree height, but the regression models did not explain the variably within the data satisfactorily. Therefore, the uniformity index calculated using the direct UAV-height values presented results close to the field inventory, reaching better results when using the second height approach (error ranging 2.8-7.8%).

Research highlights: The uniformity index using the UAV-derived height from the proposed methods was close to the values obtained in field. We noted the potential for using UAV imagery in forest monitoring.

Additional keywords: digital terrain model; forest inventory; photogrammetry; remote sensing; tree detection.

Abbreviations used: CHM (Canopy Height Model); DBH (Diameter at Breast Height); DSM (Digital Surface Model); DTM (Digital Terrain Model); GCP (Ground Control Points); NIR (Near Infrared); SfM (Structure from Motion); UAV (Unmanned Aerial Vehicle).

Introduction

The major source of wood in Brazil is commercial tree plantations, responsible for 91% of the wood production in the country in the last year (IBGE, 2015; IBÁ, 2016). These plantations are mostly composed by species of the genus *Eucalyptus* and *Pinus*, which represents, respectively, 72% and 21% of the total planted area (IBÁ, 2016), and from the total wood production, around 41% is used by the pulp and paper companies (IBGE, 2015). According to IBÁ (2016), Brazil has the best productivity rate per year for *Eucalyptus* and *Pinus* genus compared to other countries, showing an average growth rate of more than 35 m³ ha⁻¹ year⁻¹ for

Eucalyptus and around 32 m³ ha⁻¹ year⁻¹ for *Pinus*. Even with that degree of production, there is still a need for improvements in the production rates.

In order to monitor the forest production and development, forest inventories are performed to support future management planning (Scott *et al.*, 2002; Köhl *et al.*, 2006). Beside the consolidation of the forest inventory techniques, it is difficult to model the forest production, because of the variability caused by factors such as fertilization and water availability, which can affect the growing rates (Binkley *et al.*, 2002, 2010; Stape *et al.*, 2010; Otto *et al.*, 2014). In addition, the stand structure also affects the productivity, although even in stands with the same genetic material and in the same environmental conditions, the trees can present different growing rates (Binkley *et al.*, 2010; Stape *et al.*, 2010). This information is important because if the stand is too heterogeneous, the final productivity will be lower than in a more uniform stand (Luu *et al.*, 2013; Hakamada *et al.*, 2015a), even if the dominant trees show larger growth.

One of the ways to observe the uniformity in a forest it is using a forest uniformity index (UI), such as the Pvar50 (Stape *et al.*, 2006), where the accumulated contribution of the smaller trees (50%) is compared to the total of the variable being analyzed (as volume, height, biomass). The Pvar50 index is important because it can be used to compare stands with distinct production capacity, as observed by Hakamada *et al.* (2015b). For a *Eucalyptus* spp. forest to be considered uniform, the Pv50 (for volume in this case) should occur between 37-50% (Hakamada *et al.*, 2015b).

The Pvar50 index is usually calculated using a sample of the real population being analyzed, but it is still an expensive activity (Schreuder *et al.*, 1993; Gibbs *et al.*, 2007). A viable option is the use of remote sensing techniques (Holopainen & Kalliovirta, 2006; Hummel *et al.*, 2011). This technology allows the collection of information at a low price, and in some cases provides more information than traditional inventories, since it is possible to stratify the population (McRoberts & Tomppo, 2007). The use of remote sensing techniques in forest inventories has been applied for many years, including the use of Digital Aerial Photography (DAP) (Naesset, 2002; Hirschmugl *et al.*, 2007; Järnstedt *et al.*, 2012), Airbone Laser Scannig (ALS) (Oliveira *et al.*, 2012; Wallace *et al.*, 2012; Gobakken *et al.*, 2015), satellite imagery (Baltsavias *et al.*, 2008; Gebreslasie *et al.*, 2011), as well as combinations of those (St-Onge *et al.*, 2004; Koukoulas & Blackburn, 2005; Bohlin *et al.*, 2012; Garzon-Lopez *et al.*, 2013).

The development of the Unmanned Aerial Vehicles (UAVs) as a tool in the inventory process has become an option because of three important characteristics:

high-resolution and low cost compared to other remote sensing techniques, possibility of frequent monitoring, and automatic operation (Wallace *et al.*, 2012; White *et al.*, 2013; Salamí *et al.*, 2014). Recent applications has shown the possibility of using UAV-imagery as a tool to detect individual trees (Hung *et al.*, 2012; Wallace *et al.*, 2016), to identify species (Puttonen *et al.*, 2010; Lisein *et al.*, 2015), to calculate heights and crown areas (Zarco-Tejada *et al.*, 2014; Díaz-Varela *et al.*, 2015; Guerra-Hernández *et al.*, 2016; Panagiotidis *et al.*, 2016; Wallace *et al.*, 2016; Guerra-Hernández *et al.*, 2017) and even to calculate the tree growth (Dempewolf *et al.*, 2017; Goodbody *et al.*, 2017; Guerra-Hernández *et al.*, 2017; Jiménez-Brenes *et al.*, 2017).

Along with the development of the UAV systems, one other important technology was developed in this same context, called Structure from Motion (SfM), and this is the major engine behind the UAV imagery processing. The SfM was presented by Ullman (1979), and it is a group of algorithms that recover the 3D position of a scene by tracking the motion of 2D features on subsequent images with overlap (Quan, 2010; Fisher *et al.*, 2014). In addition, the SfM can also estimate the cameras' calibration parameters when they are unknown (Szeliski, 2011; Verhoeven, 2011) allowing the use of consumer cameras to create 3D models.

The aim of this study was to evaluate the utility of using UAV data to estimate the uniformity index in *Pinus taeda* L. and *Euclyptus* spp. plantations, by detecting trees and their respective heights automatically from the UAV-derived 3D point cloud.

Material and methods

Study area and data collection

Study area

In this study, we selected two commercial forest stands, one comprised by *Pinus* genus, and the second by *Eucalyptus* genus. The initial plant spacing established was approximately 2 m × 3 m in the *Pinus* stand, and 3 m × 4 m in the *Eucalyptus* stand. The sites were located in Telêmaco Borba municipality (Paraná state, Brazil), and property of the pulp and paper company, Klabin SA, which supported this study. The study area was located in a region with natural occurrence of "Campos Gerais" (General Open Fields) in the second plateau of the state (KLABIN SA, 2016), where the Cfa climate is predominantly known as subtropical with hot summers (IAPAR, 2012). The study area has an approximate altitude of 760 m above sea level (Santos, 2005), and an annual average precipitation between 1200-1600 mm (IAPAR, 2012).

The stands were located in a region with flat terrain with slope between 0-10% (ITCG, 2006).

The trees were 1.5 years old, and in the *Pinus* stand the canopy is mostly open, with the trees' crowns completely separated from the neighbor trees, while in the *Eucalyptus* stand there is partial overlap between trees in the same line, but in between the lines the ground is visible.

We delimited two plots in each stand, randomly selected, with an area of 150 m² for the *P. taeda* stand, and of 250 m² for the *Eucalyptus* spp. stand. This plot size comprises 5 lines with approximately 6 trees each, totaling an average of 30 trees in each plot. The study area location details are presented in Fig. 1.

Field data collection

The field data collection was done by measuring all trees in each plot. For each tree, the respective line and position in the line was recorded, and the height was measured using the Haglöf Electronic Clinometer. Table 1 presents statistical information about tree count and tree heights from the plots. The tree positions were measured using a GPS Pathfinder ProXRT Receiver (Trimble).

Aerial data collection

The UAV aerial data collection occurred in August 2015, when the flights and the ground control collection were performed. The flights were done in subsequent days, with clear sky and light winds (ranging from 3 to 3.5 m/s), around noon. We selected for both stands an overlap of 80% lateral and 85% longitudinal, and we covered the same area twice using perpendicular flight lines. The flight height was 150 meters, which allowed a Ground Sample Distance (GSD) of 5 cm to be obtained. The flights covered a total area of 75 ha in the *Eucalyptus* spp. stand, requiring two flights of 28 min each to cover the area with the selected options. In the *Pinus* stand we covered an area of 40 ha in one flight of 33 min. The total images collected for each flight was 380 in the *Pinus* stand, and 712 in the *Eucalyptus* stand. The flight plans were created and monitored using eMotion 2 (from Sensefly), and all images took were used in the processing, since the software controlled the image acquisition to cover only our interest area.
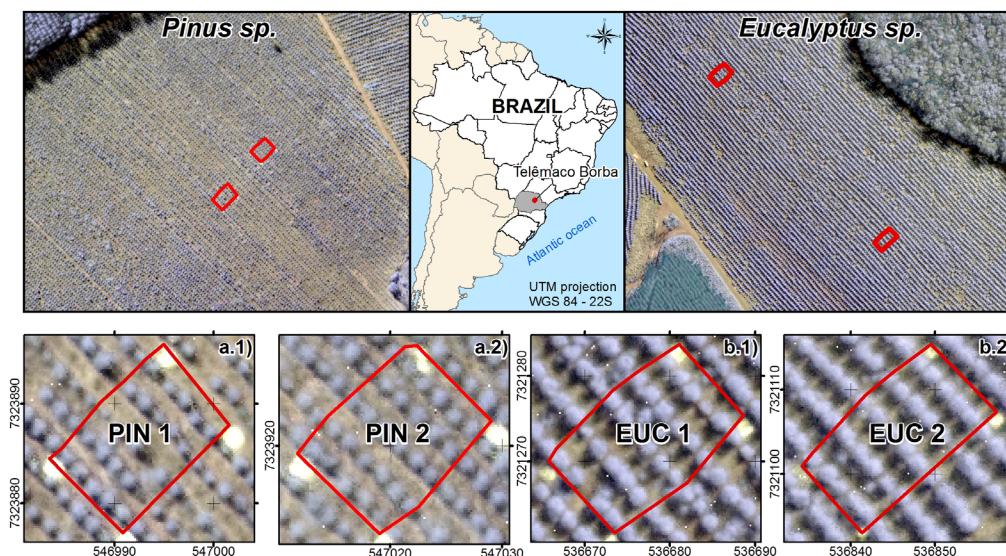
Figure 1. Study area location and plot details. (a.1, a.2) *Pinus* stand plots. (b.1, b.2) *Eucalyptus* stand plots.

Table 1. Statistical information about tree number and tree heights in *Pinus* and *Eucalyptus* plots.

Plot	Number of trees		Height (m)		
	Planted	**Survived**	**Min.**	**Max.**	**Mean (SD)**
PIN 1	31	31	2.30	3.30	2.72 (0.05)
PIN 2	30	29	0.90	3.10	2.51 (0.09)
EUC 1	32	31	1.60	3.90	3.23 (0.10)
EUC 2	29	29	2.60	4.10	3.60 (0.08)

The UAV data acquisition was done using the UAV Ebee-Ag (Sensefly company), with a Near Infrared Sensor camera (NIR) Canon PowerShot S110 (Canon company). The camera had 12 MP of resolution, the sensor size is 7.44 × 5.58 mm, and the focal distance is 4.5 mm.

Four ground control points (GCP) were positioned in each plot, located in the four corners, using a target made of paper. The paper used was white, had a square shape with 1.8 m per side, and we painted an X using black paint in the center of the paper, showing the exact center of the target. The ground control coordinates were collected using a GPS Pathfinder ProXRT Receiver, and the accuracy of the ground control points considering the mean error was: $X = 0.7 \pm \sigma X$ $0.27; Y = 0.7 \pm \sigma Y\ 0.27; Z = 1.1 \pm \sigma Z\ 0.3$. This system, in normal conditions, should provide solutions with submeter (+ 1 ppm) accuracy. The low accuracy in the ground control collection was result from problems in the collection in the day of the flights. The GPS could not find an adequate solution, and we believed this was because the area is remote, and the signal is affected by the network signal and presence of trees.

The image processing was done with the Postflight Terra 3D software (vers. 3.4.46), in which the images were externally and internally oriented using homologous points found in the images. In the Postflight, the processing is split in 3 major steps, the first where the images are calibrated internal and externally. In the first step, we selected full image scale, automatic number of keypoints, and alternative calibration (optimize all internal and external parameters). In the second step, for a dense point cloud, we selected an optimal point density, ½ image scale, and 3 minimum matches for point. In the last step we generated the DSM and orthomosaic. For the DSM, we selected the option to filter noise points, to smooth the DSM using a sharp model, and to interpolate the values using the Inverse Distance Weighting. The resolution was set as automatic for both DSM and orthomosaic. The image coordinates and the ground control points were manually inserted after the first step, and the project was reoptimized to use the coordinates as reference.

The processing took approximately 3.5 and 10 hours for the *Pinus* and *Eucalyptus* stands, respectively. The geolocation accuracy was calculated using the position of the ground control, and we obtained an absolute RMSE of 0.46 m, 1.23 m and 1.06 m on X, Y and Z coordinates in the *Pinus* stand, respectively, and 1.39 m, 2.47 m and 0.74 m in the *Eucalyptus* stand.

After the orientation process, we generated a 3D dense point cloud, an orthomosaic, and a Digital Surface Model (DSM). Research has shown that in some cases it is possible to classify the 3D point cloud and select only the points on the ground and to use these points to generate a Digital Terrain Model (DTM). The DTM generation is still limited in the photogrammetric software because the point cloud generated only represents the surface of the objects. In this work, we performed the analysis based only on the UAV-derived point cloud.
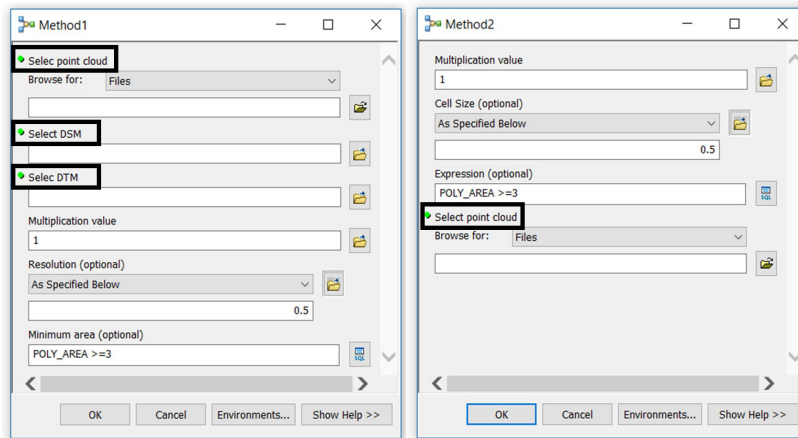
Data processing

The data processing was done applying two different methods, involving three major steps: ground point classification, tree detection, and tree heights calculation. The first step is to classify the ground points in the dense point cloud obtained from the UAV imagery processing and generate a DSM and DTM from these points. This step was only applied on Method 1. The second step is to detect the trees' positions using the spectral information stored in the point cloud, and this step is common in both methods, so the tree detection is the same in both cases. The last step is to calculate the heights, and this is where the DTM and DSM from the first step will be used in the Method 1, while in Method 2 we used the point cloud (with no classification) to generate the higher and lowest elevations values and calculate the heights. More details are presented in the next subsections.

The workflow inputs are presented in Fig. 2. The ground point classification, as well as the DTM and DSM generation for Method 1 were processed separately. The processing was done for one plot at the time. The plot's shape was used to clip the point cloud and a buffer of 10 m was included for all the plots to avoid the edge effect. The workflow applied is presented in Fig. 3.

Ground point classification

The ground point classification was done using the software SAGA (System for Automated Geoscientific Analyses) vers. 2.2 (Conrad *et al.*, 2015). The process to classify the points and generate the DTM and DSM was based on the workflow created by Wichmann *et al.* (2013), to process Lidar data in SAGA GIS.

In the workflow created by Wichmann *et al.* (2013), the point cloud is converted to two grid format files, one with the highest elevations (the DSM), and one with the lower elevations. The grid with the lower elevations is filtered to remove the non-ground points, using the DTM-filter (slope-based) algorithm based in Vosselman (2000). We selected the parameters of slope (s) and search radius (r) as 5 and 3 m to execute this tool. The points classified as ground

Figure 2. Input parameters for both methods to detect and calculate tree heights using UAV point clouds. DSM: Digital Surface Model. DTM: Digital Terrain Model.
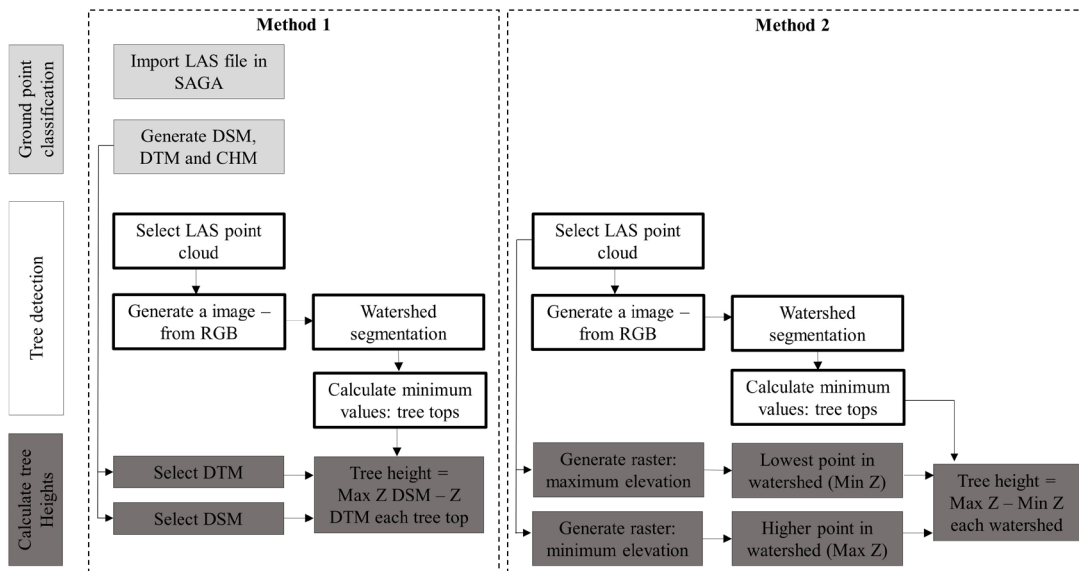
Figure 3. Processing workflow for Methods 1 and 2. DSM: Digital Surface Model. DTM: Digital Terrain Model. CHM: Canopy Height Model. LAS: Laser file format. SAGA: System for Automated Geoscientific Analyses. Min: Minimum value. Max: Maximum value. Z: Elevation.

were interpolated using the Multilevel B-Spline Interpolation (from grid) tool, created by Lee *et al.* (1997). We used a matrix with level 11. The result was smoothed using the Multi Direction Lee Filter (Lee, 1980), using 1 and 2 as absolute and relative error respectively. In all the steps performed in the SAGA GIS, we used a cell size of 0.5 m followed from LIDAR research efforts (Höfle *et al.*, 2012).

A Canopy Height Model (CHM) was also generated using the *Grid Difference* (Conrad *et al.*, 2015) tool, in which we performed a mathematical operation of subtraction to calculate the difference between the DSM and the DTM. The CHM was not used in the tree detection model, but was considered to analyze the relationship between the DSM and DTM.

Tree detection and height calculation

The process to detect the trees and calculate the heights was done using the two workflows created in ArcGIS 10.4. First, we present the tree detection, since it is the same for both methods, and later we describe the calculation of the heights.

— Tree detection. The tree detection was done using existing hydrological analysis tools developed to detect watersheds. This method, called watershed segmentation, is commonly used to delineate tree crowns, because by inverting the surface model of a forest, the crown areas are similar to small watersheds (Panagiotidis *et al.*, 2016). Usually, the watershed segmentation is applied in a CHM derived from Lidar, but in this case, we decided to use the spectral

information (RGB values) stored in the 3D point cloud.

The first step for the tree detection was the selection of the point cloud (.las file), obtained from the photogrammetric processing. An image was generated from the point cloud using the *Las dataset to Raster* tool, by selecting the option to interpolate the RGB values. The image created was multiplied by 1 or -1, using the *Times* tool. The image should be multiplied by 1 when the digital value (RGB values) on the trees positions is smaller than the digital value of the ground. When the digital value in the trees positions is higher than the soil, the image needs be multiplied by -1. To decide the value, we checked the digital values in the point cloud prior to the detection, and we inserted the right value in the workflow. This process generated an inverted image.

In the sequence, the *focal statistics* tool was applied to highlight the lowest positions. For that we used a circular search, with 2 cells radius, and we selected as output the minimum values. This process helps to smooth small differences in color within the same crown. The image smoothed was used to calculate the flow direction, using the *Flow direction* tool, and this result was applied in the *Basin* tool, which delineated watersheds in the flow direction file. In this case, the watersheds are tree areas; it includes the tree crown as well some parts of the ground surrounding each tree. We calculated the area of each tree area, and excluded the areas smaller than 3 m^2.

The position of each tree was calculated by searching the lowest value in the inverted image within each tree area. To finalize the detection, we included the number of each tree area in the tree detected points (ID number), using the tool *Intersect*, and this number was used in the height calculation, as described in the next subsection.

The field measured trees were manually plotted as shapefiles in the image generated from the RGB values in the point cloud. For this task we considered the information collected in field, as line and position of each tree in the line. Each tree received an ID number in the field, and this number was included in the shapefile.

After the detection, we made the correspondence of each detected tree with the respective field measured tree. In this step we also identified the false positive and false negative trees. The correspondence was done using a spatial join between the tree areas (the segmentation output in shapefile) with the manually plotted trees. Using the spatial join, each tree area received the identification (ID) number of the manually plotted tree. In the sequence, we made an interception of these tree areas (already with the ID number) with the detected trees. With this process, each detected tree that does not have the ID number of the field tree is

a false positive. On the other hand, if a detected tree has two ID numbers, it means that two tree crowns are merged in the segmentation, therefore, one tree was not detected. In this case, we kept the ID of the closest field tree, and the missing tree was considered a false negative.

The tree detection errors were calculated using the following equations:

$$FP\ error\ (\%) = \frac{FP * 100}{TF}$$
$$FN\ error\ (\%) = \frac{FN * 100}{TF}$$

where FP error (%) = percentage of false positive detected trees; FN error (%) = percentage of false negative detected trees; FN = total of false negative detected trees; FP = total of false positive detected trees; TF = total of trees measured in field.

— Height calculation – Method 1. In Method 1 we selected the DSM and DTM (generated using SAGA) as input in the workflow, as well as the point cloud needed to detect the trees positions. In this method, after the tree detection, the value Z of each tree position in the DTM was calculated using the tool *Add Surface Information*. We calculated the tree top as the maximum Z value for each tree area in the DSM. The height was calculated as being the subtraction of the Z in the DSM and the Z in the DTM for each tree area.

— Height calculation – Method 2. The tree height calculation in Method 2 was similar to Method 1, but instead of using the DSM and DTM generated from SAGA, we extracted the necessary values from the point cloud. To accomplish this, the point cloud was transformed in two raster files, one with the lowest elevation values for cell, and the other with the highest elevation values. These files were created using the *Las dataset to Raster* tool, selecting the Elevation as field to be interpolated, and selecting the cell assignment as Minimum and Maximum. The process was done using the tool twice, one time to obtain the minimum values (Grid Minimum), and in the other to obtain the maximum values (Grid Maximum).

The height was calculated by searching the elevation value (Z maximum) in the Grid Maximum for each tree area, using the *Add Surface Information* tool. Next, we searched for the minimum value in the Grid Minimum for each tree area (Z minimum), using the *Zonal statistics* tool, and keeping the values for each tree area, considering the ID number. The difference between the Z maximum and Z minimum for the same tree area was considered the tree height. Details about the difference on tree height calculation from both methods are presented in Fig. 4.
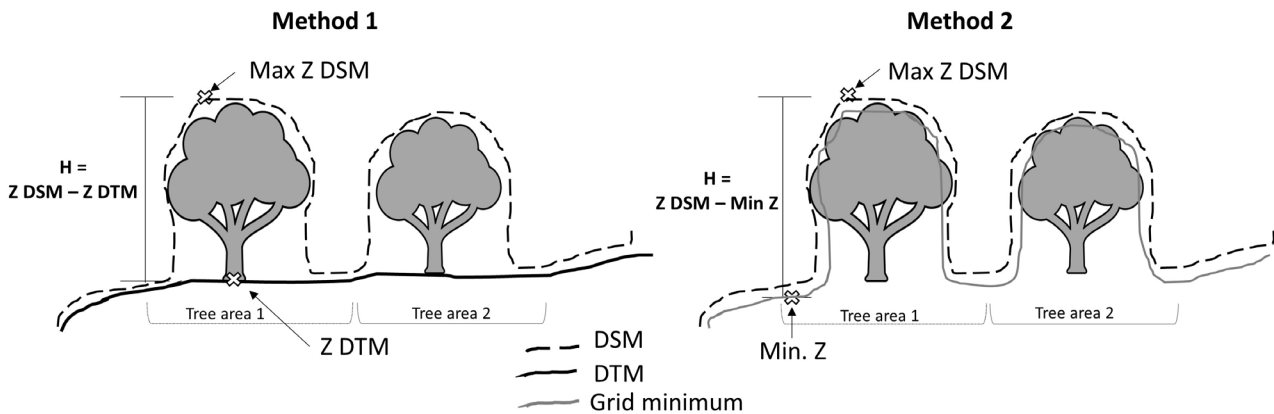
Figure 4. Difference in tree height calculation (UAV-height) between Method 1 and 2. DSM: Digital Surface Model. DTM: Digital Terrain Model.

In general, the difference between the methods is that in Method 2 we did not classify the point cloud, therefore we did not have a DTM. To be able to calculate the tree height without the DTM, we searched the minimum elevation values within the same tree area, and we expected that the results of this method were similar to the method using the DTM, considering that the terrain is relatively flat and there is ground visible between the trees.

The UAV-height values for both methods were compared to the field values, applying an Analysis of variance (ANOVA), and a Tukey Significant Difference test, both with 95% confidence level.

Tree height estimation

Tree height was estimated using linear regression modeling in the R (R Core Team, 2016). We used the UAV-derived tree height (UAV-height) as a predictor of field tree heights (field-H). Considering the regression assumptions (linearity, independence, homoscedasticity of error, and normality distribution of the error) we fit a linear regression model. The models were created for each stand, using the values of the two plots in each.

Uniformity index estimation

The stand uniformity was estimated using the $PH^3 50$ index, which is a variation of the PV50, usually applied to evaluate uniformity in plantations. According to Hakamada (2012), the $PH^3 50$ presents a high correlation with the PV50, so it can be used in young stands, when it is not possible to obtain the DBH (Diameter at Breast Height -1.3 m).

The $PH^3 50$ was obtained according to the following equation:

$$PH^3 50 = \frac{\sum_{k=1}^{n/2} H^3}{\sum_{k=1}^{n} H^3}$$

where $PH^3 50$ = accumulated participation of the 50% smallest trees heights; H^3 = cubic power of the ith tree height; n = sorted tree number (smallest to largest).

The $PH^3 50$ index was calculated using the field data, the calculated heights (from the two methods tested), and the estimated heights (from the mathematic equations). In the cases where the methods identified a nonexistent tree (a commission error), or did not detect one or more trees (omission error), we calculated the $PH^3 50$ considering the number of detected trees. This was done since in a real application it will not be possible to detect if these errors happen. In the $PH^3 50$ the real number of trees was considered from the field data.

Results

Ground point classification

The statistical analysis of the generated products from the point cloud classification in SAGA is presented in Table 2, as well the parameters observed in the original point cloud. As detailed in the data processing, this process was only applied in Method 1.

The DSM values correspond to the maximum values observed in the point cloud, while the DTM values correspond to the minimum values, as expected. The *Pinus* and *Eucalyptus* stands have distinct characteristics regarding the density of points generated, which is much higher in the *Eucalyptus* stand. The maximum values in the CHM (*i.e.* the tree tops) also vary between the two stands. We found maximum values of 3.10-4.42 m in the *Pinus* stand, and 4.66-6.24 m in the *Eucalyptus* stand.

In Fig. 5 the digital models (DSM, DTM and CHM) are presented for each plot. Close to the edges of the

Table 2. Basic information about the files generated from the point cloud classification, applied in Method 1.

File [1]	Z min.	Z max.	Z av.	Z min.	Z max.	Z av.
	PIN 1			PIN 2		
DSM	819.15	825.55	822.35	822.99	829.67	826.33
Ground points	818.56	823.12	820.84	822.54	826.80	824.67
Objects	819.01	824.16	821.59	823.01	827.61	825.31
DTM	818.33	823.67	821.00	822.75	827.19	824.97
CHM	0.03	4.42	2.23	-0.03	3.10	1.54
Point cloud	818.51	825.55	822.03	822.54	829.67	826.11
Point count (total / points/m²)	130,680 / 95.35			146,167 / 98.45		
	EUC 1			EUC 2		
DSM	730.27	736.74	733.51	722.33	728.40	725.37
Ground points	729.39	734.04	731.72	721.31	725.20	723.26
Objects	729.91	734.99	732.45	721.82	726.34	724.08
DTM	725.41	734.68	730.05	720.45	725.63	723.04
CHM	-0.03	6.24	3.11	0.17	4.66	2.42
Point cloud	729.39	736.74	733.07	721.31	728.40	724.85
Point count (total / points/m²)	308,929 / 150.94			433,689 / 223.46		

[1] DSM = digital surface model; Ground points = all points classified as being on the ground; Objects = all the points classified as not being part of the ground, but being any other structure as trees; DTM = digital terrain model; CHM = canopy height model. Point cloud = the original point cloud considering all the point classes. Z min., Z max. and Z av. = minimum, maximum and average elevation values, respectively.
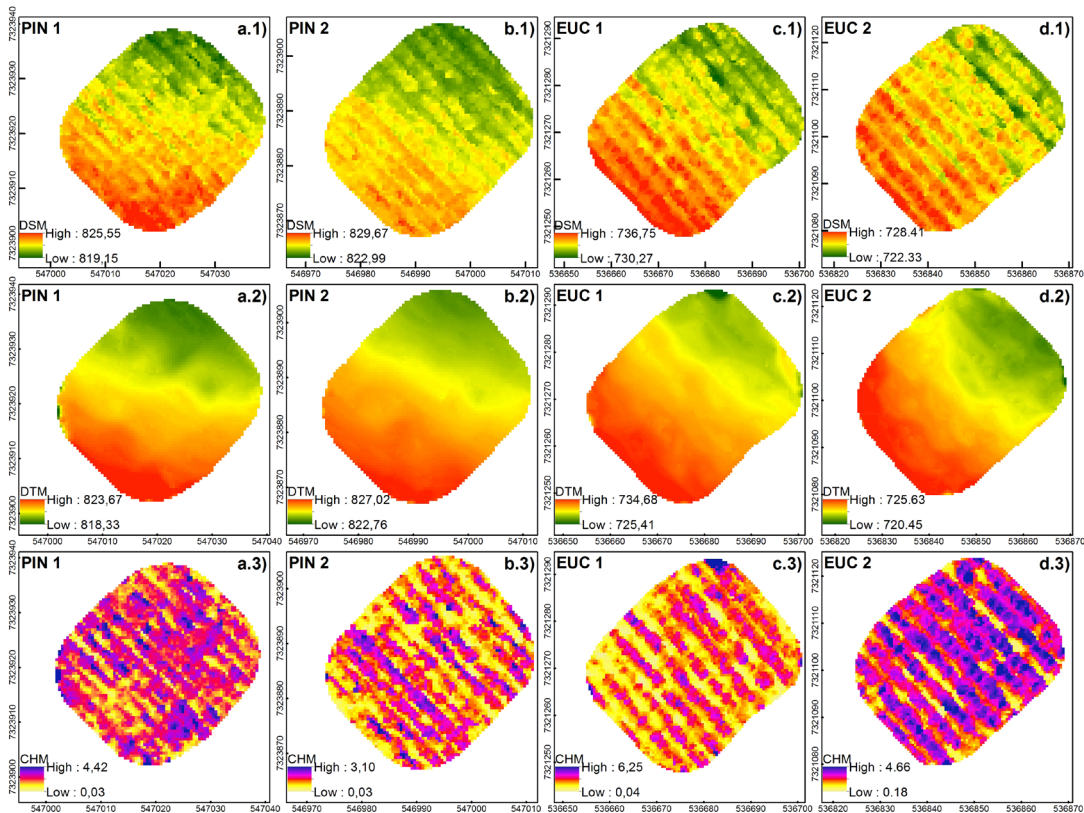
Figure 5. Digital models generated using the point cloud classification in SAGA GIS for Method 1. EUC: Eucalyptus spp. trees. PIN: *Pinus taeda* trees. a), b), c) and d) are, respectively, the plots PIN 1, PIN 2, EUC 1 and EUC 2. 1), 2) and 3) are, respectively, the DSM, DTM and CHM of each plot.

plots, we observed some altitude values extremely low or high in the DTM. These values are errors and happen because the algorithm uses a neighborhood relationship. This situation was expected, and it did not interfere with the rest of the processing since we included a margin of a 10 m buffer.

In Table 3 and Fig. 6 we can observe the relationship between altitude values (Z) calculated in the DTMs and observed in the field survey (GPS). We can observe a strong relationship for both plots (Fig. 6), even if the error presented an average value of 1.07 m and 0.87 m for *Pinus* and *Eucalyptus* stands respectively. The values from the *Eucalyptus* stand in the DTM were closer to the field data than in the *Pinus* stand.

Tree detection

The process applied to detect the trees in the plots was the same for both Method 1 and Method 2, therefore the detection results are the same. The results are presented in Fig. 7, as well as in Table 4.

In general, we noticed that almost all the trees were detected using the proposed method, showing only error between 1-2 trees per plot (maximum error 6.45%). We also noticed that in the *Pinus* plots the trees' positions are dislocated from the tree top, and the trees' positions were calculated as being in the tree shadow. Besides the displacement in the tree position, this did not affect the height results, since the heights are calculated using the maximum value in the DSM of each tree area.

Regression models and tree height estimative

The tree height was estimated using UAV-height (from Method 1 and Method 2) and field measurements of tree height. The UAV-heights are presented in Table 5. We can observe that the

Eucalyptus spp. trees (EUC) are taller than the *Pinus taeda* (PIN), reaching 4.10 m of maximum height, while the *Pinus taeda* have a maximum of 3.30 m. Considering the ANOVA and Tukey tests, both methods are statistically different to the field measurements.

We observed that in all plots, the UAV-derived height values underestimated the field tree heights in most of the cases. Therefore, we decided to try to model the field tree height instead of using the direct UAV extracted height as the true tree height. The relationship between UAV and field height, for both stands and methods, is presented in Fig. 8. The regression model showed no statistically significant correlation (r of 0.23 and 0.12 for Methods 1 and 2, respectively) for the *Pinus* stand, therefore the regression was not able to explain the variations (R^2 of 0.04 and 0.00 for Methods 1 and 2, respectively).

In the *Eucalypus* stand the results are better, since the correlations between the UAV-height and measured height were statistically significant, and classified as moderate (r=0.54) or strong (r=0.71), according to Andriotti (2003). Therefore, the regression models were only able to explain part of the variation on the data, obtaining R^2 values of 0.37 and 0.49 for Methods 1 and 2, respectively. Considering the regression quality, we decided to use the direct UAV-height to calculate the uniformity index.

Table 3. DTM validation from GCPs on *Pinus* and *Eucalyptus* stands.

Metric (n=8)	*Pinus* stand	*Eucalyptus* stand
Mean difference (m)	1.07	0.87
Standard deviation of difference (m)	0.19	0.15
Median difference (m)	1.15	0.94
Minimum difference (m)	0.41	0.34
Maximum difference (m)	1.89	1.35
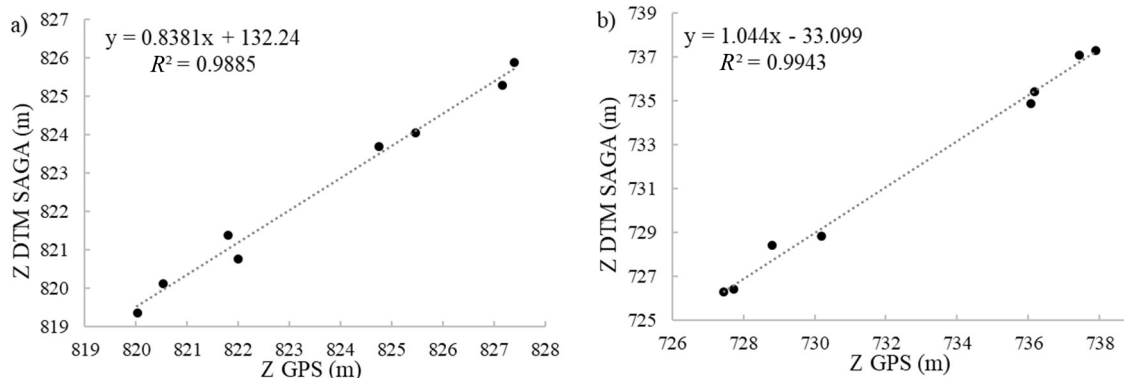
Figure 6. Validation of DTM values using the GCPs coordinates for *Pinus* (a) and *Eucalyptus* (b) stands.
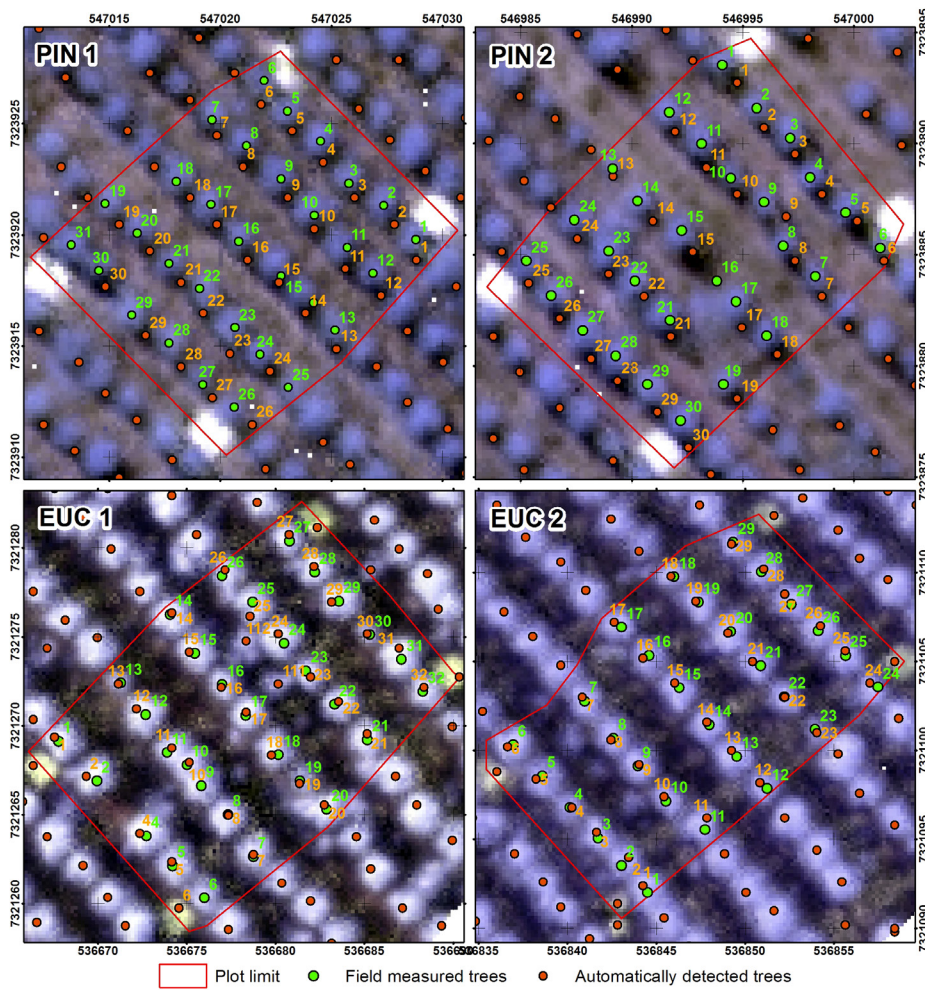
Figure 7. Automatically detected and field measured trees. EUC: *Eucalyptus* spp. trees.
PIN: *Pinus taeda* trees.

Table 4. Detected and field measured trees. Values between parenthesis are the % variation based in the total field measured trees.

Plot [1]	Total - field	Total of detected trees	False negative detected	False positive detected
PIN 1	31	29	2 (6.45%)	0
PIN 2	29	28	1 (3.44%)	0
EUC 1	31	32	1 (3.22%)	2 (6.25%)
EUC 2	29	29	0 (0%)	0

[1] PIN = *Pinus taeda* trees. EUC = *Eucalyptus* spp. trees.

Table 5. Tree heights UAV-height and filed measured values.

Stand	Measurement	Mean	SD	Minimum	Maximum	Samples (trees)
Eucalyptus	Field	3.41[a]	0.53	1.60	4.10	60
	Method 1	2.45[c]	0.59	1.02	3.44	61
	Method 2	3.15[b]	0.63	1.40	4.22	61
Pinus	Field	2.62[a]	0.39	0.90	3.30	60
	Method 1	1.73[c]	0.25	1.26	2.37	57
	Method 2	2.32[b]	0.32	1.36	2.98	57

SD = standard deviation. Different letters indicate significant differences obtained through Tukey test.
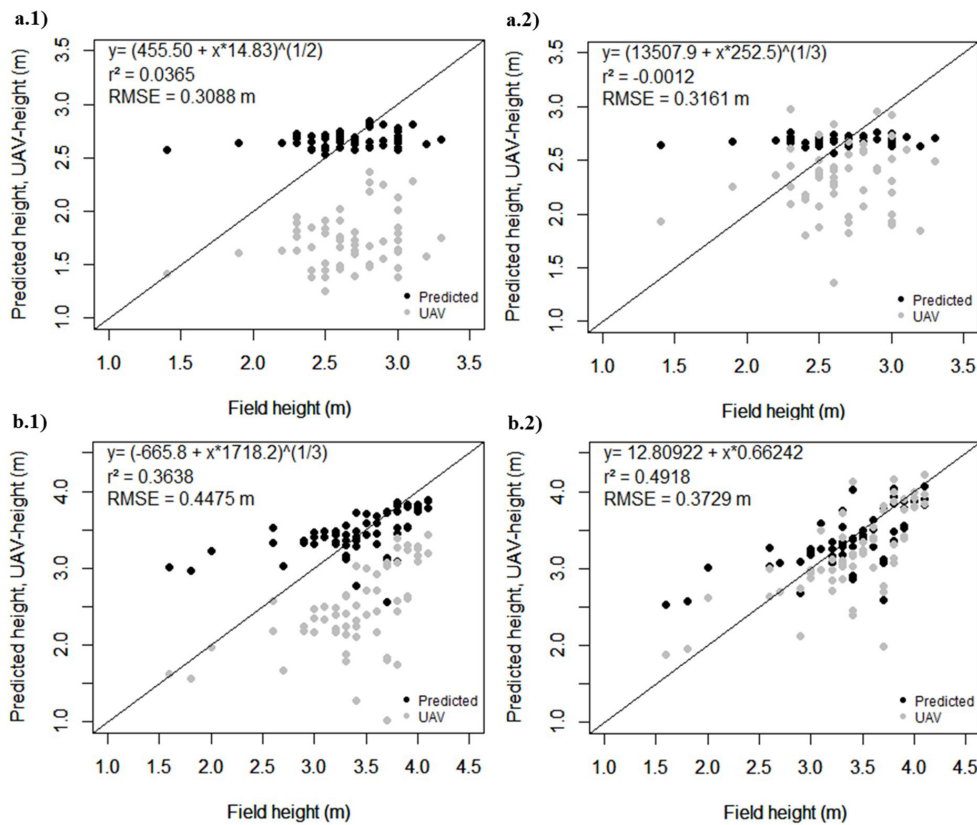
Figure 8. Relationship between UAV-height, field-height and predicted height, in *Pinus* (a) and *Eucalyptus* (b) stands for Methods 1 (.1) and 2 (.2).

Uniformity index – PH³50

The calculated PH³50 values using the field measurements (Field-height), and the values obtained from the images processing (UAV-height), for the two processing methods, are presented in Table 6.

The PH³50 calculated from Method 2 presented better results, with errors ranging between 2.79-7.86%, while the Method 1 had large errors, mostly in the plots PIN 2 and EUC 1. However, the results in the other two plots were satisfactory (Table 5). With the exception of the Method 1 in the plot PIN 1, and the PH³50 calculated by the method underestimated the PH³50 obtained in the field. The field-PH³50 in all the plots are between the

interval of 37-50% delimited by Hakamada *et al.* (2015b) as values where the stands can be considered uniform.

Discussion

Considering the tree detection results observed in this study, it is possible to conclude the importance of the UAV technology in monitoring young forest stands. The UAV data collected using passive sensors was capable of automatically measure the trees' positions and heigths allowing the reduction of the cost of traditional forest inventories or Lidar surveys (White *et al.*, 2013; Hernández-Clemente *et al.*, 2014). The workflow created can be easily applied in other early stands to identify possible high rates of variation in the growing among plants in the stands. This is important because when the plants are still young, the responses of fertilization and other silvicultural practices are more pronounced since tree growth declines with age (Borders *et al.*, 2004; Martínez-Vilalta *et al.*, 2007). In cases where growth is extremely irregular the replacement of the current species for another variety that is more productive can be a viable option.

Table 6. PH³50 uniformity index values. Values between parentheses are the error (%)

Plot [1]	Field	UAV - Method 1	UAV - Method 2
PIN 1	0.4051	0.4135 (-2.07)	0.3938 (2.79)
PIN 2	0.3618	0.2817 (22.14)	0.3418 (5.53)
EUC 1	0.3460	0.2883 (16.68)	0.3188 (7.86)
EUC 2	0.3513	0.3210 (8.63)	0.3319 (5.52)

[1] PIN = *Pinus taeda* trees. EUC = *Eucalyptus* spp. trees.

Even with the tree detection being able to reach almost 100% of the trees, it is still important to consider the potential problems with detection. One of these problems is the presence of shadows in the images which can create an error in the tree's position. Occlusions caused by shadows could be problematic for generation of image-based point clouds, especially in dense forest canopies (Baltsavias *et al.*, 2008; Ke *et al.*, 2010; Laliberte *et al.*, 2010; White *et al.*, 2013; Dandois *et al.*, 2015). This problem can be minimized in some cases by image collection in specific weather conditions (White *et al.*, 2013; Dandois *et al.*, 2015; Näsi *et al.*, 2015).

Our results about tree detection are similar to observations regarding adult *Eucalyptus* trees (Wallace *et al.*, 2016). Díaz-Varela *et al.* (2015) found comparable results in individual and hedgerow olive trees using UAV data. Using UAVs is close and/or more accurate than detection of trees in high resolution satellite images (Zhou *et al.*, 2013) and traditional aerial flights (Hirschmugl *et al.*, 2007; St-Onge *et al.*, 2015; Tanhuanpää *et al.*, 2016). In our results we also observed some commission errors (when objects that are not trees are detected as if they are), and that is possibly a reflection of the fine resolution used, as observed by Ke & Quackenbush (2011).

In this study, we were also able to observe the possibility of DTM generation from the UAV data and calculate tree heights. Even without the availability of a DTM source to use for comparison, we believe that the DTM generation is possible in the conditions as presented where the tree canopies are not closed, as observed by Guerra-Hernández *et al.* (2016, 2017) and Jensen & Mathews (2016). The visual analysis of the DSM and DTM generated and values observed in other studies using Lidar and GPS values as reference, as in Dandois & Ellis (2013), Zahawi *et al.* (2015), Jensen & Mathews (2016) and Wallace *et al.* (2016), helped us reach that conclusion. Jensen & Mathews (2016) observed that the DTM derived of UAV images overestimated the ground height compared to Lidar derived DTM, but was able to calculate tree heights with a similar accuracy as those obtained with Lidar data.

The calculated tree height presented good correlation with the field measurements only for the *Eucalyptus* spp. stand, while in the *Pinus taeda* correlation was not significant. The result for the *Eucalyptus* spp. stand was similar to observations made by Dandois & Ellis (2013), Hernández-Clemente *et al.* (2014) and Díaz-Varela *et al.* (2015), but below the values observed by Guerra-Hernández *et al.* (2016), Panagiotidis *et al.* (2016), Wallace *et al.* (2016) and Guerra-Hernández *et al.* (2017). In both stands, the tree height calculated from

the UAV data underestimated the field measured values, especially for coniferous trees, as usually observed in photogrammetric measurements from traditional DAP and photogrammetric methods (Naesset, 2002; Korpela, 2004; St-Onge *et al.*, 2004; Tanhuanpää *et al.*, 2016) and from UAV-imagery and SfM (Díaz-Varela *et al.*, 2015; Cunliffe *et al.*, 2016; Panagiotidis *et al.*, 2016).

One possible explanation for the problems with the height calculation is based on the theory presented by Lisein *et al.* (2013) and also observed by Díaz-Varela *et al.* (2015). They noted that the CHMs derived from images underestimate heights (compared to Lidar CHM) more frequently in areas with object discontinuities such as isolated trees. Lisein *et al.* (2013) also observed specific problems in coniferous stands with low density. In our case, we observed tree height underestimation in both stands and since the trees in both cases are isolated (because the canopies are discontinuous), we believe that the CHM smoothed the tree top heights. Another point that can be observed is presented by Zahawi *et al.* (2015), which observed high correlation between measured and UAV estimated heights in trees in general, but found weak correlation in small trees (1.5-4 m), possibly due to the small height variance as well as to the altitude errors in the DTM in the low trees' positions according to the authors. In our database, the *Pinus taeda* stand presents smaller trees and the point cloud density in that stand is considerably smaller than in the *Eucalyptus* spp. stand.

Another problem that needs to be addressed is the low accuracy of the GCP used in this study, considering that the equipment used should provide a better solution, and the errors in the geolocation of the UAV products are probably related to the poor GCP accuracy. Our geolocation errors, with RMSE ranging from 0.46-2.47 m are much large than the values observed on other studies using also an eBee UAV and similar topography conditions, as Guerra-Hernández *et al.* (2017) that observed a RMSE <5 cm with 5 GCPs, and < 2 cm with 10 GCPs, and the mean error of 2 cm using 6 GCPs observed by Birdal *et al.* (2017). Our RMSE values are also higher than observed for authors using rotary wings UAVs, as 0.31 m of mean error using 8 GCPs observed by Jensen & Mathews (2016), and <7 cm using 9 GCPs observed by Tomaštík *et al.* (2017). Also, it is possible that the location of our GCPs was not optimal, since they were placed in the corner of the plots and did not covered the total area of the stand. The low geolocation accuracy is believed to be one of the major issues in our measurements, since authors observed the necessity to employ correct control points (considering number, positioning and adequate equipment) to transform the relative reference from the images to a

metric coordinate system (Westoby *et al.*, 2012; Nex & Remondino, 2014; Mesas-Carrascosa *et al.*, 2015, 2016; Carvajal-Ramírez *et al.*, 2016; Gašparović *et al.*, 2017; Raczynski, 2017; Tomaštík *et al.*, 2017).

One interesting point to note is the improved result from Method 2 in comparison with Method 1. In Method 1 we used a DTM as a source of the minimum tree height, while in Method 2 we searched for the smallest elevation inside the delineated tree crown, which was found to be better. This could result from an overestimation of the terrain in the DTM, as observed by Dandois & Ellis (2013), Jensen & Mathews (2016) and Guerra-Hernández *et al.* (2017), or the result of the lack of ground points around the trees' canopies.

The lack of points under canopy results in an underestimation of the terrain, as observed by Wallace *et al.* (2016), but it is possible that in the present case some points close to the trees, such as leaves in the ground, could lead the algorithm to overestimate the terrain under the canopies. According to Cunliffe *et al.* (2016) that can happen because photogrammetric techniques have problems modeling the extremity of the plants. The authors proposed to use other metrics besides the maximum height as a predictor of tree heights. Similar results, in the metric selection, were observed by Lisein *et al.* (2013), Hernández-Clemente *et al.* (2014), Díaz-Varela *et al.* (2015), Zahawi *et al.* (2015) and Panagiotidis *et al.* (2016). Hernández-Clemente *et al.* (2014) observed that the 90th percentile of the height presented a better prediction of the total tree height, reaching an R^2 value of 0.67, compared to the R^2 of 0.50 reached by the maximum height.

The uniformity index calculated for the plots using the calculated heights showed good results, thus it is possible that the errors in the measurements are mostly punctual variations. It is difficult to use a model for individual trees, but the results are satisfactory in the plot level. In a similar situation, Zucon *et al.* (2015) applied UAV imagery to calculate the Pvar50 in a young *Eucalyptus* stand using the crown area and observed good results despite having some problems in the correct crown delineation.

Considering the presented results, there is a large potential for the application of UAV data in forest growth monitoring that have been demonstrated by a few recent UAV studies in different forest ecosystems (Dempewolf *et al.*, 2017; Goodbody *et al.*, 2017; Guerra-Hernández *et al.*, 2017). Our results are satisfactory with consideration of the existing limitations of this technology, as the dependence of another source for terrain elevation in closed vegetation (Mathews & Jensen, 2013; Wallace *et al.* 2016), as well the lack of methods for DTM generation specific for UAV imagery, where there is not an uniform point distribution (Dandois & Ellis, 2013).

Other limitations that should be considered are the importance of the flying conditions and the camera's quality. The camera quality in low-cost UAV is usually poor and the cameras are not calibrated, which can cause a great amount of distortion in the images and affect the accuracy of the products (Salamí *et al.*, 2014; Puliti *et al.*, 2015). The knowledge of the distortions caused can be corrected in many cases, or can be compensated by the advantages, such as the high resolution, offered by the UAV technology (Whitehead & Hugenholtz, 2014). The aerial data acquisition requires more control since it is important that the flights are always carried out in conditions of equal luminosity and with higher overlaps, including the need to fly more than the selected area to avoid edge distortions (Mathews & Jensen, 2013; Whitehead & Hugenholtz, 2014; Dandois *et al.*, 2015).

Conclusions

In this study, we observed the potential of point clouds derived from UAV imagery to monitor the growing uniformity in forest stands using a uniformity index based on the trees' heights. Our results suggest that this technology can be applied with good results.

Preferred results were observed in tree detection, but some problems remained in estimating the heights. Underestimation of the tree heights was observed in all evaluated situations, with distinct results in the stands, leading to the conclusion that the results cannot be generalized without caution, since differences in the tree stand characteristics leads to different results on the uniformity index.

The DTM generation using the UAV-derived point cloud was also evaluated and the results are promising. Based on our results and the review of the literature, we believe DTM generation is possible in some specific situations, but in many cases, that is not possible with acceptable error tolerances. In these cases, the use of UAV to calculate heights is still dependent on the availability of some terrain model from another source. We suggest for future studies a more complete evaluation of the stand characteristic to be performed for the tree height estimation since we observed large differences in the stands.

We also suggest that this process could have better results if more accurate and maybe a larger number of ground control were applied, since the low accuracy of the GCP was probably one of the major sources of errors in the tree heights. Also, improvements in the image processing could also lead to better results, mostly considering the availability of new software and tools in the existing photogrammetric software to classify ground points.

Acknowledgement

References

Andriotti JLS, 2003. Fundamentos de Estatística e Geoestatística. UNISINOS, São Leopoldo.

Baltsavias E, Gruen A, Eisenbeiss H, Zhang L, Waser LT, 2008. High-quality image matching and automated generation of 3D tree models. Int J Remote Sens 29: 1243-1259. https://doi.org/10.1080/01431160701736513

Binkley D, Stape JL, Ryan MG, Barnard HR, Fownes J, 2002. Age-related decline in forest ecosystem growth: An individual-tree, stand-structure hypothesis. Ecosystems 5: 58-67. https://doi.org/10.1007/s10021-001-0055-7

Binkley D, Stape JL, Bauerle WL, Ryan MG, 2010. Explaining growth of individual trees: Light interception and efficiency of light use by Eucalyptus at four sites in Brazil. For Ecol Manage 259: 1704-1713.

Birdal AC, Avdan U, Türk T, 2017. Estimating tree heights with images from an unmanned aerial vehicle. Geomatics, Nat Hazards Risk 8: 1144-1156. https://doi.org/10.1080/19475705.2017.1300608

Bohlin J, Wallerman J, Fransson JES, 2012. Forest variable estimation using photogrammetric matching of digital aerial images in combination with a high-resolution DEM. Scand J For Res 27: 692-699. https://doi.org/10.1080/02827581.2012.686625

Borders BE, Will RE, Markewitz D, Clark A, Hendrick R, Teskey RO, Zhang Y, 2004. Effect of complete competition control and annual fertilization on stem growth and canopy relations for a chronosequence of loblolly pine plantations in the lower coastal plain of Georgia. For Ecol Manage 192: 21-37.

Carvajal-Ramírez F, Agüera-Vega F, Martínez-Carricondo PJ, 2016. Effects of image orientation and ground control points distribution on unmanned aerial vehicle photogrammetry projects on a road cut slope. J Appl Remote Sens 10: 34004. https://doi.org/10.1117/1.JRS.10.034004

Conrad O, Bechtel B, Bock M, Dietrich H, Fischer E, Gerlitz L, Wehberg J, Wichmann V, Böhner J, 2015. System for Automated Geoscientific Analyses (SAGA) v. 2.1.4. Geosci Model Dev 8: 1991-2007. https://doi.org/10.5194/gmd-8-1991-2015

Cunliffe AM, Brazier RE, Anderson K, 2016. Ultra-fine grain landscape-scale quantification of dryland vegetation structure with drone-acquired structure-from-motion photogrammetry. Remote Sens Environ 183: 129-143. https://doi.org/10.1016/j.rse.2016.05.019

Dandois JP, Ellis EC, 2013. High spatial resolution three-dimensional mapping of vegetation spectral dynamics using computer vision. Remote Sens Environ 136: 259-276. https://doi.org/10.1016/j.rse.2013.04.005

Dandois JP, Olano M, Ellis EC, 2015. Optimal altitude, overlap, and weather conditions for computer vision uav estimates of forest structure. Remote Sens 7: 13895-13920. https://doi.org/10.3390/rs71013895

Dempewolf J, Nagol J, Hein S, Thiel C, Zimmermann R, 2017. Measurement of within-season tree height growth in a mixed forest stand using UAV imagery. Forests 8: 1-15. https://doi.org/10.3390/f8070231

Díaz-Varela R, de la Rosa R, León L, Zarco-Tejada P, 2015. High-resolution airborne UAV imagery to assess olive tree crown parameters using 3D photo reconstruction: Application in breeding trials. Remote Sens 7: 4213-4232. https://doi.org/10.3390/rs70404213

Fisher RB, Breckon TP, Dawson-Howe K, Fitzgibbon A, Robertson C, Trucco E, Williams CKI, 2014. Dictionary of computer vision and image processing, 2nd Ed. Chichester.

Garzon-Lopez CX, Bohlman SA, Olff H, Jansen PA, 2013. Mapping tropical forest trees using high-resolution aerial photographs. Biotropica 45: 308-316. https://doi.org/10.1111/btp.12009

Gašparović M, Seletković A, Berta A, Balenović I, 2017. The evaluation of photogrammetry-Based DSM from low-cost UAV by LiDAR-based DSM. South-East Eur For 8: 117-125. https://doi.org/10.15177/seefor.17-16

Gebreslasie MT, Ahmed FB, van Aardt JAN, Blakeway F, 2011. Individual tree detection based on variable and fixed window size local maxima filtering applied to IKONOS imagery for even-aged Eucalyptus plantation forests. Int J Remote Sens 32: 4141-4154. https://doi.org/10.1080/01431161003777205

Gibbs HK, Brown S, Niles JO, Foley JA, 2007. Monitoring and estimating tropical forest carbon stocks: making REDD a reality. Environ Res Lett 2: 45023. https://doi.org/10.1088/1748-9326/2/4/045023

Gobakken T, Bollandsås OM, Næsset E, 2015. Comparing biophysical forest characteristics estimated from photogrammetric matching of aerial images and airborne laser scanning data. Scand J For Res 30: 73-86. https://doi.org/10.1080/02827581.2014.961954

Goodbody TRH, Coops NC, Marshall PL, Tompalski P, Crawford P, 2017. Unmanned aerial systems for precision forest inventory purposes: A review and case study. For Chron 93: 71-81.

Guerra-Hernández J, González-Ferreiro E, Sarmento A, Silva JJ, Nunes A, Correia AC, Fontes L, Tomé M, Díaz-Varela R, Guerra-Hernandez J, et al., 2016. Using high resolution UAV imagery to estimate tree variables in *Pinus pinea* plantation in Portugal. Forest Syst 25 (2): 1-5. https://doi.org/10.5424/fs/2016252-08895

Guerra-Hernández J, González-Ferreiro E, Monleón VJ, Faias SP, Tomé M, Díaz-Varela RA, 2017. Use of multi-temporal UAV-derived imagery for estimating individual tree growth in *Pinus pinea* stands. Forests 8: 1-19. https://doi.org/10.3390/f8080300

Hakamada RE, 2012. Uso do inventário florestal como ferramenta de monitoramento da qualidade silvicultural em povoamentos clonais de *Eucalyptus.* Master dissertation. São Paulo University, Luiz de Queiroz College of Agriculture, Piracicaba.

Hakamada RE, Stape JL, de Lemos CCZ, Almeida AEA, Silva LF, 2015a. Uniformidade entre árvores durante uma rotação e sua relação com a produtividade em *Eucalyptus* clonais. Cerne 21: 465-472. https://doi.org/10.1590/01047760201521031716

Hakamada RE, Stape JL, De Lemos CCZ, Almeida AEA, Silva LF, 2015b. Uso do inventário florestal e da uniformidade entre árvores como ferramenta de monitoramento da qualidade silvicultural em plantios clonais de eucalipto. Sci For Sci 43: 27-36.

Hernández-Clemente R, Navarro-Cerrillo RM, Romero Ramírez FJ, Hornero A, Zarco-Tejada PJ, 2014. A novel methodology to estimate single-tree biophysical parameters from 3D digital imagery compared to aerial laser scanner data. Remote Sens 6: 11627-11648. https://doi.org/10.3390/rs61111627

Hirschmugl M, Ofner M, Raggam J, Schardt M, 2007. Single tree detection in very high resolution remote sensing data. Remote Sens Environ 110: 533-544. https://doi.org/10.1016/j.rse.2007.02.029

Höfle B, Hollaus M, Hagenauer J, 2012. Urban vegetation detection using radiometrically calibrated small-footprint full-waveform airborne LiDAR data. ISPRS J Photogramm Remote Sens 67: 134-147. https://doi.org/10.1016/j.isprsjprs.2011.12.003

Holopainen M, Kalliovirta J, 2006. Modern data acquisition for forest inventories. In: Forest inventory: Methodology and applications; Kangas A & Maltamo M (eds.), pp: 343-362. Springer Netherlands, Dordrecht. https://doi.org/10.1007/1-4020-4381-3_21

Hummel S, Hudak AT, Uebler EH, Falkowski MJ, Megown KA, 2011. A comparison of accuracy and cost of LiDAR versus stand exam data for landscape management on the Malheur National Forest. J For 109: 267-273.

Hung C, Bryson M, Sukkarieh S, 2012. Multi-class predictive template for tree crown detection. ISPRS J Photogr Remote Sens 68: 170-183. https://doi.org/10.1016/j.isprsjprs.2012.01.009

IAPAR, 2012. Cartas climáticas do Estado do Paraná. Instituto Agroômico do Paraná.

IBÁ, 2016. Relatório Anual. Industria Brasileira de Árvores [Brazilian Tree Industry].

IBGE, 2015. Produção da extração vegetal e da silvicultura. Instituto Brasileiro de Geografia e Estatística.

ITCG, 2006. Mapa de declividade do Parana. Instituto de Terras Cartografia e Geociencias.

Järnstedt J, Pekkarinen A, Tuominen S, Ginzler C, Holopainen M, Viitala R, 2012. Forest variable estimation using a high-resolution digital surface model. ISPRS J Photogr Remote Sens 74: 78-84. https://doi.org/10.1016/j.isprsjprs.2012.08.006

Jensen JLR, Mathews AJ, 2016. Assessment of image-based point cloud products to generate a bare earth surface and estimate canopy heights in a woodland ecosystem. Remote Sens 8 (1): 50. https://doi.org/10.3390/rs8010050

Jiménez-Brenes FM, López-Granados F, Castro AI de, Torres-Sánchez J, Serrano N, Peña JM, 2017. Quantifying pruning impacts on olive tree architecture and annual canopy growth by using UAV-based 3D modelling. Plant Methods 13: 1-15. https://doi.org/10.1186/s13007-017-0205-3

Ke Y, Quackenbush LJ, 2011. A review of methods for automatic individual tree-crown detection and delineation from passive remote sensing. Int J Remote Sens 32: 4725-4747. https://doi.org/10.1080/01431161.2010.494184

Ke Y, Quackenbush LJ, Im J, 2010. Synergistic use of QuickBird multispectral imagery and LIDAR data for object-based forest species classification. Remote Sens Environ 114: 1141-1154. https://doi.org/10.1016/j.rse.2010.01.002

Klabin SA, 2016. Resumo Público - Plano de manejo Florestal 2016.

Köhl M, Magnussen S, Marchetti M, 2006. Sampling methods, remote sensing and GIS multiresource forest inventory. Springer-Verlag, NY, 387pp. https://doi.org/10.1007/978-3-540-32572-7

Korpela I, 2004. Individual tree measurements by means of digital aerial photogrammetry, Vol 3. Edition. The Finnish Society of Forest Science, 93 pp.

Koukoulas S, Blackburn GA, 2005. Mapping individual tree location, height and species in broadleaved deciduous forest using airborne LIDAR and multi-spectral remotely sensed data. Int J Remote Sens 26: 431-455. https://doi.org/10.1080/0143116042000298289

Laliberte AS, Herrick JE, Rango A, Winters C, 2010. Acquisition, orthorectification, and object-based classification of unmanned aerial vehicle (UAV) imagery for rangeland monitoring. Photogr Eng Remote Sens 76: 661-672. https://doi.org/10.14358/PERS.76.6.661

Lee JS, 1980. Digital image enhancement and noise filtering by use of local statistics. IEEE Trans Pattern Anal Mach Intell. https://doi.org/10.1109/TPAMI.1980.4766994

Lee S, Wolberg G, Shin SY, 1997. Scattered data interpolation with multilevel b-splines. IEEE Trans Vis Comput Graph 3: 228-244. https://doi.org/10.1109/2945.620490

Lisein J, Pierrot-Deseilligny M, Bonnet S, Lejeune P, 2013. A photogrammetric workflow for the creation of a forest canopy height model from small unmanned aerial system

imagery. Forests 4: 922-944. https://doi.org/10.3390/f4040922

Lisein J, Michez A, Claessens H, Lejeune P, 2015. Discrimination of deciduous tree species from time series of unmanned aerial system imagery. PLoS One 10: 1-20. https://doi.org/10.1371/journal.pone.0141006

Luu TC, Binkley D, Stape JL, 2013. Neighborhood uniformity increases growth of individual Eucalyptus trees. For Ecol Manage 289: 90-97.

Martínez-Vilalta J, Vanderklein D, Mencuccini M, 2007. Tree height and age-related decline in growth in Scots pine (*Pinus sylvestris* L.). Oecologia 150: 529-544. https://doi.org/10.1007/s00442-006-0552-7

Mathews AJ, Jensen JLR, 2013. Visualizing and quantifying vineyard canopy LAI using an unmanned aerial vehicle (UAV) collected high density structure from motion point cloud. Remote Sens 5: 2164-2183. https://doi.org/10.3390/rs5052164

McRoberts RE, Tomppo EO, 2007. Remote sensing support for national forest inventories. Remote Sens Environ 110: 412-419. https://doi.org/10.1016/j.rse.2006.09.034

Mesas-Carrascosa FJ, García MDN, De Larriva JEM, García-Ferrer A, 2016. An analysis of the influence of flight parameters in the generation of unmanned aerial vehicle (UAV) orthomosaicks to survey archaeological areas. Sensors 16 (11): 1838. https://doi.org/10.3390/s1611183

Mesas-Carrascosa FJ, Torres-Sánchez J, Clavero-Rumbao I, García-Ferrer A, Peña JM, Borra-Serrano I, López-Granados F, 2015. Assessing optimal flight parameters for generating accurate multispectral orthomosaicks by uav to support site-specific crop management. Remote Sens 7: 12793-12814. https://doi.org/10.3390/rs71012793

Naesset E, 2002. Determination of mean tree height of forest stands by digital photogrammetry. Scand J For Res 17 (5): 37-41. https://doi.org/10.1080/028275802320435469

Näsi R, Honkavaara E, Lyytikäinen-Saarenmaa P, Blomqvist M, Litkey P, Hakala T, Viljanen N, Kantola T, Tanhuanpää T, Holopainen M, 2015. Using UAV-based photo-grammetry and hyperspectral imaging for mapping bark beetle damage at tree-level. Remote Sens 7: 15467-15493. https://doi.org/10.3390/rs71115467

Nex F, Remondino F, 2014. UAV for 3D mapping applications: A review. Appl Geomatics 6: 1-15. https://doi.org/10.1007/s12518-013-0120-x

Oliveira LT de, Carvalho LMT de, Ferreira MZ, Oliveira TC de A, Junior FWA, 2012. Application of LIDAR to forest inventory for tree count in stands of *Eucalyptus* sp. Cerne 18: 175-184. https://doi.org/10.1590/S0104-77602012000200001

Otto MSG, Hubbard RM, Binkley D, Stape JL, 2014. Dominant clonal *Eucalyptus grandis* x *urophylla* trees use water more efficiently. For Ecol Manage 328: 117-121.

Panagiotidis D, Abdollahnejad A, Surový P, Chiteculo V, 2016. Determining tree height and crown diameter from high-resolution UAV imagery. Int J Remote Sens 38: 2392-2410. https://doi.org/10.1080/01431161.2016.1264028

Puliti S, Olerka H, Gobakken T, Næsset E, 2015. Inventory of small forest areas using an unmanned aerial system. Remote Sens 7: 9632-9654. https://doi.org/10.3390/rs70809632

Puttonen E, Litkey P, Hyyppä J, 2010. Individual tree species classification by illuminated-Shaded area separation. Remote Sens 2: 19-35. https://doi.org/10.3390/rs2010019

Quan L, 2010. Image based modeling. Springer, NY, 257 pp. https://doi.org/10.1007/978-1-4419-6679-7

R Core Team, 2016. R: A language and environment for statistical computing. R Foundation for Statistical Computing, Vienna.

Raczynski RJ, 2017. Accuracy analysis of products obtained from UAV-borne photogrammetry influenced by various flight parameters. Master thesis. Norwegian University of Science and Technology, Trondheim.

Salamí E, Barrado C, Pastor E, 2014. UAV flight experiments applied to the remote sensing of vegetated areas. Remote Sens 6: 11051-11081. https://doi.org/10.3390/rs61111051

Santos JC, 2005. Plano Diretor de Desenvolvimento de Telêmaco Borba. Telêmaco Borba.

Schreuder HT, Gregoire TG, Wood GB, 1993. Sampling methods for multiresource forest inventory. John Wiley & Sons, NY, 446 pp.

Scott CT, Gove JH, Scott CT, Gove JH, 2002. Forest inventory. In: Encyclopedia of environmetrics. pp: 814-820. John Wiley & Sons, Ltd, Chichester, UK.

St-Onge B, Jumelet J, Cobello M, Véga C, 2004. Measuring individual tree height using a combination of stereophotogrammetry and lidar. Can J For Res 34: 2122-2130. https://doi.org/10.1139/x04-093

St-Onge B, Audet FA, Bégin J, 2015. Characterizing the height structure and composition of a boreal forest using an individual tree crown approach applied to photogrammetric point clouds. Forests 6: 3899-3922. https://doi.org/10.3390/f6113899

Stape JL, Rocha JC, Donatti Z, 2006. Indicadores de qualidade silvicultural na Aracruz: 2000 a 2005. Piracicaba.

Stape JL, Binkley D, Ryan MG, Fonseca S, Loos RA, Takahashi EN, Silva CR, Silva SR, Hakamada RE, Ferreira JM de A, *et al.*, 2010. The Brazil eucalyptus potential productivity project: Influence of water, nutrients and stand uniformity on wood production. For Ecol Manage 259: 1684-1694.

Szeliski R, 2011. Computer vision: Algorithms and applications. Springer, 824 pp. https://doi.org/10.1007/978-1-84882-935-0

Tanhuanpää T, Saarinen N, Kankare V, Nurminen K, Vastaranta M, Honkavaara E, Karjalainen M, Yu X, Holopainen M, Hyyppa J, *et al.*, 2016. Evaluating the performance of high-altitude aerial image-based digital

surface models in detecting individual tree crowns in mature boreal forests. Forests 7 (7): 143. https://doi.org/10.3390/f7070143

Tomaštík J, Mokroš M, Saloš S, Chudỳ F, Tunák D, 2017. Accuracy of photogrammetric UAV-based point clouds under conditions of partially-open forest canopy. Forests 8 (5): 151. https://doi.org/10.3390/f8050151

Ullman S, 1979. The interpretation of structure from motion. Proc R Soc London 203: 405-426. https://doi.org/10.1098/rspb.1979.0006

Verhoeven G, 2011. Taking computer vision aloft - Archaeological three-dimensional reconstructions from aerial photographs with photoscan. Archaeol Prospect 62: 61-62. https://doi.org/10.1002/arp.399

Vosselman G, 2000. Slope based filtering of laser altimetry data. Int Archiv Photogr Remote Sens 33 (B3/2): 678-684.

Wallace L, Lucieer A, Watson C, Turner D, 2012. Development of a UAV-LiDAR system with application to forest inventory. Remote Sens 4: 1519-1543. https://doi.org/10.3390/rs4061519

Wallace L, Lucieer A, Malenovsky Z, Turner D, Vopenka P, 2016. Assessment of forest structure using two UAV techniques: A comparison of airborne laser scanning and structure from motion (SfM) point clouds. Forests 7: 1-16. https://doi.org/10.3390/f7030062

Westoby MJ, Brasington J, Glasser NF, Hambrey MJ, Reynolds JM, 2012. "Structure-from-Motion" photogrammetry: A low-cost, effective tool for geoscience applications. Geomorphology 179: 300-314. https://doi.org/10.1016/j.geomorph.2012.08.021

White JC, Wulder MA, Vastaranta M, Coops NC, Pitt D, Woods M, 2013. The utility of image-based point clouds for forest inventory: A comparison with airborne laser scanning. Forests 4: 518-536. https://doi.org/10.3390/f4030518

Whitehead K, Hugenholtz CH, 2014. Remote sensing of the environment with small unmanned aircraft systems (UASs), part 1: A review of progress and challenges. J Unmanned Veh Syst 2: 86-102. https://doi.org/10.1139/juvs-2014-0007

Wichmann V, Conrad O, Jochem A, 2013. LiDAR point cloud processing with SAGA GIS. Hamburg Beiträge zur Phys Geogr und Landschaftsökologie 20: 81-90.

Zahawi RA, Dandois JP, Holl KD, Nadwodny D, Reid JL, Ellis EC, 2015. Using lightweight unmanned aerial vehicles to monitor tropical forest recovery. Biol Conserv 186: 287-295. https://doi.org/10.1016/j.biocon.2015.03.031

Zarco-Tejada PJ, Diaz-Varela R, Angileri V, Loudjani P, 2014. Tree height quantification using very high resolution imagery acquired from an unmanned aerial vehicle (UAV) and automatic 3D photo-reconstruction methods. Eur J Agron 55: 89-99. https://doi.org/10.1016/j.eja.2014.01.004

Zhou J, Proisy C, Descombes X, le Maire G, Nouvellon Y, Stape JL, Viennois G, Zerubia J, Couteron P, 2013. Mapping local density of young Eucalyptus plantations by individual tree detection in high spatial resolution satellite images. For Ecol Manage 301: 129-141.

Zucon ARS, Hawkes B, Lemos CCZ de, 2015. Use of unmanned aerial vehicle images as a tool to evaluate stand uniformity in clonal Eucalyptus plantations. Anais do XVII Simpósio Bras Sensoriamento Remoto - SBSR, João Pessoa INPE 6381-6388.